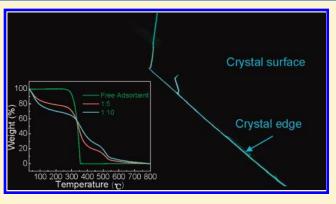# High-Quality Large-Size Organic Crystals Prepared by Improved Physical Vapor Growth Technique and Their Optical Gain Properties

Jie Yang,[†] Hong-Hua Fang,[†] Ran Ding,[†] Shi-Yang Lu,[†,‡] Yong-Lai Zhang,[†] Qi-Dai Chen,[†,*] and Hong-Bo Sun[†,‡,*]

[†]State Key Laboratory on Integrated Optoelectronics, College of Electronic Science and Engineering, Jilin University, 2699 Qianjin Street, Changchun 130012, China,

[‡]College of Physics, Jilin University, 119 Jiefang Road, Changchun 130023, China

ABSTRACT: We have developed an improved physical vapor transport method. This method enables us to decrease the sublimation temperature of small organic molecules, and slow the weight loss process, and then regulate the degree of vapor saturation of materials. Large-size single-crystalline materials with high quality are successfully prepared from small organic functional molecules. The slice crystals are found to be single crystalline with high quality. The surface morphologies and structural information of grown crystals were characterized by optical microscope, atomic force microscopy (AFM), and X-ray diffraction (XRD) analysis. The results indicate that the growth mechanism of single crystals is a 2D nucleation, with elementary steps, large straight steps, and layer-by-layer growth.

1. INTRODUCTION

Over past few years, organic single crystalline materials have attracted a great deal of research interest in the optoelectronic or photonic field because of their high stimulated cross sections, large and ultrafast nonlinear responses, and broad spectral tunability. Various devices, such as organic field-effect transistors (OFETs),[1−8] light-emitting transistors (LETs),[9,10] optically pumped organic semiconductor lasers (OSLs),[11−13] and upconversion lasers[14−19] based on the organic crystals have been demonstrated. Their long-range order not only reveals the performance limits of organic semiconductor materials but also provides unique insight into their intrinsic optoelectronic properties.[4] The devices of single crystals also usually have higher electronic transport properties and more excellent optical properties than those based on amorphous or polycrystalline thin films. However, surface morphologies and lattice defects of the crystals[20−22] heavily affect the performance of organic single crystal devices because the conductive channels existing in several molecular layers on the surface and the defects may serve as carrier traps. Accordingly, to achieve the highest possible performance the crystals must have the flat surface and smallest possible number of defects.

For the organic crystals' growth, melt[23−25] and solution[26,27] techniques are most common. However, the former is only applicable to organic molecules with a sufficient thermal stability, whereas the latter is limited to low growth rates and solvent or solution inclusion problems. The physical vapor transport (PVT)[28−31] is well-known to overcome these problems and is one of the most facile and feasible method for preparing crystals of high purity and lattice perfection. The principle of the physical vapor method is as follows:[28,29] the source material placed in the source tube of the reactor is heated to higher temperature; then sublimated molecules under the carrier gas transport move to a lower temperature zone and the crystal growth occurs in the crystal growth tube within a narrow temperature range. Nucleation control[32−34] is required so that growth of a smaller number of nuclei into larger crystals occurs without intergrowth. There are several parameters that have influence on the nuclei process, such as temperature distribution, inert-gas flow, and the interactions between the molecules in the crystals and so on. Besides these, the degree of vapor saturation[35] is one of the predominant factors in controlling the nuclei process, and then the quality of the products. Source temperature regulation is a way to control the vapor saturation. However, it is not very easy to find the right point to bring an appropriate degree of vapor saturation. High temperature often makes the nucleation so numerous that no well-formed crystals can be obtained and low temperature usually leads to low growth rates and even sublimation stops.[28]

In this study, we have improved the conventional physical vapor method by introducing the adsorbent (neutral aluminum oxide) in horizontal PVT growth apparatus. With the help of neutral aluminum oxide, the degree of vapor saturation was readily regulated to be an appropriate value. Large-size and flat single crystals could be prepared with this method. The

adsorbents were proved to be indispensable in improving the quality of the as-fabricated organic crystals.

2. EXPERIMENTAL SECTION

The model compound used in our work is 1,4-bis(4-methyl-styryl)benzene (BSB-Me) (Figure 2), a typical optoelectronic functional material,[36,37] which was purchased from Tokyo Chemical Industry Co., Ltd. and was used without further treatment. Besides the BSB-Me, frequently used thiophene/phenylene co-oligomer materials,[38−42] such as 2,5-bis(4-biphenylyl)thiophene (BP1T) and 5,5′-bis(4-biphenylyl)-2,2′-bithiophene (BP2T), were also grown by this improved method. The apparatus for the preparation of the crystals are very similar with that reported in the literature, as displayed in Figure 1. Neutral aluminum oxide and organic materials were mixed uniformly with certain weight/weight ratios through grinding and subsequently put into a quartz boat. The quartz boat loaded with the mixture was then put into the center of a quartz tube, which was inserted into the high temperature zone of the tube furnace. The high-purity nitrogen was adopted as a carrier and to prevent the organic materials from being oxidized. The gas flowing rate was kept at 50 mL/min.

The as-prepared organic crystals were characterized by X-ray diffraction (The diffraction experiments were carried out on a
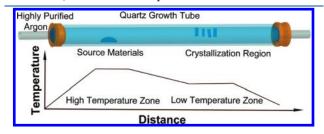

Figure 1. Schematics of the crystal growth apparatus for the physical vapor transport method, and the temperature gradient in the experiment.
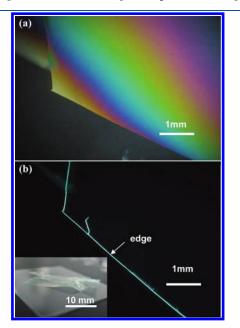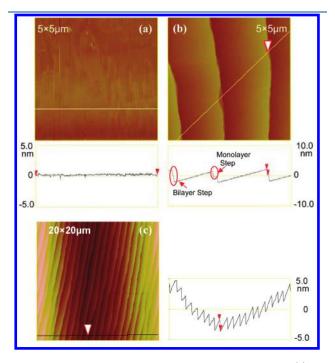

Figure 2. Optical photographs of a typical single crystal of BSB-Me grown by the adsorbent-assisted physical vapor method under the polarizing (a) and fluorescence (b) microscopy. Insert: the molecular structure of BSB-Me in (a), BSB-Me crystal under daylight lamp in (b).
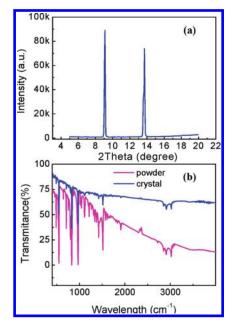
Rigaku R-AXIS RAPID diffractometer (D/max-rA, using Cu Kα radiation of wavelength 1.542 Å)), Fourier transform infrared spectroscopy (Thermo Scientific, Nicolet 6700), AFM images were recorded in the tapping mode with a Nanoscope IIIa scanning probe microscope from Digital Instruments under ambient conditions. The weight loss speeds of materials and that mixed with adsorbents were measured using thermal gravity analysis (TGA, PE TGA-7) in a nitrogen atmosphere with a heating rate of 2 °C/min. In the stimulated emission experiment, a regenerative amplifier (Spitfire, Spectra Physics) seeded with a mode-locked Ti:sapphire laser (Tsunami, Spectra Physics) generated laser pulses of about 120 fs, and a wavelength of 800 nm was used, and the second harmonic generation was the pump source. The energy of excited pulse can be controlled by neutral density filters, and the beam of excite laser was expanded first and then focused with a cylindrical lens.

3. RESULTS AND DISCUSSION

3.1. Morphology and Lattice Structure of the Grown Crystals. Large thin film crystals with a smooth surface are obtained by the improved PVT method. Neutral aluminum oxide and BSB-Me were mixed uniformly with about 30:1 ratios. The sizes and diameters of the as-prepared thin film crystals are largely dependent on the preparation conditions, such as deposition time and temperature. Larger size and thicker crystals could be obtained by adding more total of the prepared source materials and prolonging growing time. The crystals are colorless and transparent under a daylight lamp (insert of part b of Figure 2). The photoluminescence is emitted from the borders of the sample (or from some cracks on its surface), whereas the crystal surface is dark (part b of Figure 2). This indicates that the emitting transition moment is mainly polarized along the normal to the surface and the emission is self-waveguided toward the edges. The tapping mode of AFM had been used to observe the
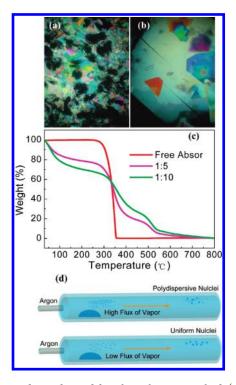

Figure 3. AFM height images of the thin film crystal at center (a) and edge (b) of the surfaces, and their cross-section analyses.

Figure 4. (a) XRD patterns of a typical single crystal of BSB-Me, (b) FTIR spectra of BSB-Me powder and BSB-Me single crystals.

central flat face with scanning range 5×5 μm and the edge of slice crystal surfaces with scanning range 20×20 μm. From the AFM height images of these crystals (part c of Figure 3), step-like morphologies existed in most of the regions on the surface edge have been found. According to their cross-section analysis, the average height of steps observed on the crystal surface edge is about 1.86 nm. However, the AFM experiment on the other regions for the BSB-Me crystals surface edge was conducted, and we found that similar step-like morphology, of which the average height of steps is about 3.9 nm, contains two smaller-steps with about 1.86 nm height in the contour line (part b of Figure 3), revealing the existence of bilayer structures. In the central area, the surface is very flat (part a of Figure 3). The X-ray diffraction pattern of the thin crystals is shown in part a of Figure 4. As can be seen, the diffraction peaks occur equidistantly with varying angle degree, the baselines of the XRD patterns is straight, and the diffraction peaks are very sharp, so these slice crystals should have good ordered layer structures. The experimentally determined cell parameters as obtained from the Cambridge Structural Database (CSD) and the unit cell parameters are $a = 7.36$ Å, $b = 5.88$ Å, $c = 38.95$ Å; $\alpha = 90°$, $\beta = 90°$, $\gamma = 90°$. According to the Bragg equation, we can calculate that the thickness of one molecular layer is 1.86 nm. Then the smaller step-heights from the AFM results are considered with the single layer of molecules. From the results for AFM morphologies and X-ray diffraction patterns, we could conclude that these crystals have the characteristics of layer-by-layer structures and each layer corresponds to a molecular monolayer. These steps (about 1.86 nm) are BSB-Me monolayers and we conclude that they are elementary steps. In the PVT method grown crystal, the molecules in the gas are combined with the ones in the crystal surface by intermolecular interactions to release the system energy. Thus, the interactions between the molecules are the main driving force of crystal formation. Zeng et al.[43] studied the growth of pentacene single crystals and found that, in the crystal growth period, there is a 2D nucleation process on the surface of pentacene. The elementary straight steps will be quickly formed from the nucleus after the
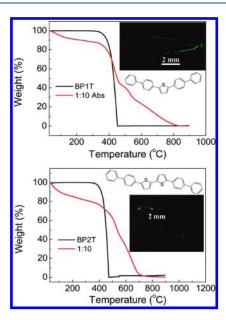

Figure 5. Products obtained by physical vapor method (a) free of absorbent and (b) with assistance of adsorbents. (c) TGA plots of pure BSB-Me powder, a mixture of BSB-Me and aluminum oxide. (d) Growth mechanisms of the as-deposited BSB-Me thin film crystals with and without the assistance of adsorbents.

2D nucleus is formed. Then the elementary steps coalesce to form large straight steps and the crystal grows by tangential movement of step trains and layer-by-layer deposition. The possible reason of the bilayer structures for BSB-Me in some regions may be similar with that of pentacene crystal. These BSB-Me monolayers can be considered as elementary steps, and each large step is formed from the piling of elementary steps.

In the absorbent-free PVT method, the productions at different temperatures (by changing the temperature of the high temperature zone from the $260 - 285$ °C) are also investigated. Part a of Figure 5 shows a typical image of the production obtained at $T_H = 270$ °C, under the polarization microscopy. It can be found that single crystals can also be obtained. However, there are many polycrystalline (shapeless and floccular) solids, which are black in the image, on the crystal surface; whereas the shapeless and floccular solids are almost eliminated when the mixture of neutral aluminum oxide and BSB-Me is used as source materials. Part b of Figure 5 shows the production obtained from the mixture at a ratio of about 5:1. The contrast indicates that the adsorbents are proven to play an important role in improving the quality of the thin film crystals.

3.2. Thermal Properties and the Role of Neutral Aluminum Oxide. The effect of the absorbents was further investigated with TGA measured in a nitrogen atmosphere. The TGA plots of BSB-Me powder and the mixtures of BSB-Me/neutral aluminum oxide with different the w/w ratio are plotted in [42]part c of Figure 5, in which the weights ratios are normalized as 100% for comparison. It can be observed from the slopes of the plots that the introduction of neutral aluminum oxide can slow the weight loss process of BSB-Me remarkably in the temperature arrange $(260-350$ °C). And the slope can be easily regulated by different

Figure 6. TGA plots of pure BP1T (a) and BP2T (b) powder, a mixture of the materials with aluminum oxide. Insert: the photograph and molecular structure of BP1T (a) and BP2T (b).

Figure 7. (a) Normalized light emission spectra of a BSB-Me single crystal under and above the threshold, (b) FWHM and PL peak intensity of a BSB-Me single crystal as a function of the incident laser energy intensity.

w/w ratios, then control the degree of vapor saturation readily. TGA also reveals that the introduction of neutral aluminum oxide (adsorbents) decreased the sublimation temperature of BSB-Me. No catalyst was adopted and no droplets were found on the surface of the crystals. FTIR also shows no chemical reaction occurs in the crystal growth process (part b of Figure 4). This method can be also applied to other materials, such as thiophene/phenylene co-oligomers, and so forth. Figure 6 shows the TGA results with assistance of adsorbents and a typical photograph of the crystals grown by the adsorbent-assisted physical vapor method for BP1T and BP2T. It can be observed that the introduction of adsorbent (neutral aluminum oxide) can slow the weight loss process and then control the degree of vapor saturation of the two materials around their sublimate temperature.

The growth of the crystals should be mainly controlled by a vapor—solid (VS) process. When the sources of organic molecules/adsorbent mixtures are heated to the deposition temperature, the molecules are sublimated to bring an appropriate degree of vapor saturation via the adsorption—desorption equilibrium. In comparison, when the sources are free of adsorbents, as illustrated in part a of Figure 5, a high flux of vapor can result in nucleation so numerous during the initial stages and therefore obtain polydispersive and no well-formed products. It is worthy of note that, by conventional methods, it is difficult to regulate the vapor saturation degree. Here, we not only controlled the vapor saturation degree but also effectively reduced the sublimate temperature.

3.3. Amplified Spontaneous Emission from the Flexible Crystals. With this method, a centimeter-sized crystal with higher quality could be prepared, whereas it retains the same photophysical properties as that grown from the conventional method. The prepared BSB-Me crystals exhibit very good flexibility and can be repeatedly bent by the external force without fracture. To obtain an in-depth characterization of optical gain properties of the crystals, the amplified spontaneous emission (ASE) was investigated. The thin film BSB-Me crystal was glued to the quartz substrate. Under the UV lamp, the edges of the crystal give stronger emission as compared with the body
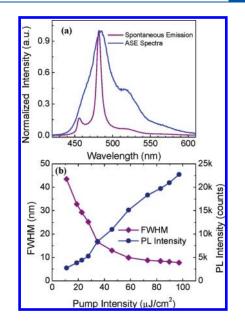
surface, as shown in part b of Figure 2, which indicates that the self-waveguided emission occurs in the crystals.[14,44,45] The light emitted at the excited region is confined inside the crystal and propagated along the thin film crystal, then radiated from the edges. Part a of Figure 7 shows the spectrum taken at below and above the threshold. The spectrum obtained with low pump energy is initially broad (~45 nm). As the incident laser fluency increases, the emission peak intensity exponentially grows, accompanied by narrowing, which are typical characteristics that stimulated emission has occurred (part b of Figure 7). The FWHM obtained was 10 nm. The relationship between the peak intensity and the pump energy was not linear, being characterized as ASE caused by stimulated emission. From the relationship between the PL intensity versus the pump fluence, the threshold could be easily concluded to be 25 μJcm^{-2}. The above results demonstrated that these crystals could be used as promising laser media. This, combined with their lightweight and flexible properties, makes BSB-Me promising candidates for portable flexible devices, such as a flexible laser or a flexible amplifier.

4. CONCLUSIONS

In summary, single crystalline materials were successfully prepared from small organic functional molecules, including bisstyrylbenzene derivatives and thiophene/phenylene co-oligomers, with the adsorbent-assisted PVT method. It has been demonstrated that the adsorbents not only control the vapor saturation degree but also effectively reduce the sublimate temperature. This enables us to produce the large-size organic thin single crystals with high quality. The primary results indicate that this improved method have the potential application for organic crystal devices applications.

■ AUTHOR INFORMATION

Corresponding Author
*Tel: +86-0431-85168281, fax: +86-431-8516-8270, E-mail: chenqd@jlu.edu.cn (Q.-D.C.); hbsun@jlu.edu.cn (H.-B.S.) (http://www.lasun-jlu.cn/new/home.php).

■ REFERENCES

(1) Mas-Torrent, M.; Durkut, M.; Hadley, P.; Ribas, X.; Rovira, C. *J. Am. Chem. Soc.* **2004**, *126*, 984.

(2) Liu, S. H.; Wang, W. C. M.; Briseno, A. L.; Mannsfeld, S. C. E.; Bao, Z. N. *Adv. Mater.* **2009**, *21*, 1217.

(3) Briseno, A. L.; Mannsfeld, S. C. B.; Shamberger, P. J.; Ohuchi, F. S.; Bao, Z. N.; Jenekhe, S. A.; Xia, Y. N. *Chem. Mater.* **2008**, *20*, 4712.

(4) Reese, C.; Bao, Z. N. *J. Mater. Chem.* **2006**, *16*, 329.

(5) Tang, Q. X.; Jiang, L.; Tong, Y. H.; Li, H. X.; Liu, Y. L.; Wang, Z. H.; Hu, W. P.; Liu, Y. Q.; Zhu, D. B. *Adv. Mater.* **2008**, *20*, 2947.

(6) Kimura, Y.; Niwano, M.; Ikuma, N.; Goushi, K.; Itaya, K. *Langmuir* **2009**, *25*, 4861.

(7) Braga, D.; Campione, M.; Borghesi, A.; Horowitz, G. *Adv. Mater.* **2010**, *22*, 424.

(8) Jurchescu, O. D.; Subramanian, S.; Kline, R. J.; Hudson, S. D.; Anthony, J. E.; Jackson, T. N.; Gundlach, D. J. *Chem. Mater.* **2008**, *20*, 6733.

(9) Bisri, S. Z.; Takenobu, T.; Yomogida, Y.; Shimotani, H.; Yamao, T.; Hotta, S.; Iwasa, Y. *Adv. Funct. Mater.* **2009**, *19*, 1728.

(10) Nakanotani, H.; Saito, M.; Nakamura, H.; Adachi, C. *Adv. Funct. Mater.* **2010**, *20*, 1610.

(11) Fujiwara, S.; Bando, K.; Masumoto, Y.; Sasaki, F.; Kobayashi, S.; Haraichi, S.; Hotta, S. *Appl. Phys. Lett.* **2007**, *91*.

(12) Sasaki, F.; Kobayashi, S.; Haraichi, S.; Fujiwara, S.; Bando, K.; Masumoto, Y.; Hotta, S. *Adv. Mater.* **2007**, *19*, 3653.

(13) Fang, H. H.; Chen, Q. D.; Yang, J.; Wang, L.; Jiang, Y.; Xia, H.; Feng, J.; Ma, Y. G.; Wang, H. Y.; Sun, H. B. *Appl. Phys. Lett.* **2010**, *96*.

(14) Fang, H. H.; Chen, Q. D.; Yang, J.; Xia, H.; Ma, Y. G.; Wang, H. Y.; Sun, H. B. *Opt. Lett.* **2010**, *35*, 441.

(15) Fang, H. H.; Chen, Q. D.; Yang, J.; Xia, H.; Gao, B. R.; Feng, J.; Ma, Y. G.; Sun, H. B. *J. Phys. Chem. C* **2010**, *114*, 11958.

(16) Fang, H.; Yang, J.; Ding, R.; Wang, L.; Xia, H.; Feng, J.; Ma, Y.; Sun, H. *Appl. Phys. Lett.* **2010**, *97*, 101101.

(17) Fang, H.; Xu, B.; Chen, Q.; Ding, R.; Chen, F.; Yang, J.; Wang, R.; Tian, W.; Feng, J.; Wang, H. *IEEE J. Quan. Electron.* **2010**, *46*, 1775.

(18) Fang, H.; Chen, Q.; Ding, R.; Yang, J.; Ma, Y.; Wang, H.; Gao, B.; Feng, J.; Sun, H. *Opt. Lett.* **2010**, *35*, 2561.

(19) Xia, H.; Yang, J.; Fang, H.; Chen, Q.; Wang, H.; Yu, X.; Ma, Y.; Jiang, M.; Sun, H. *Chemphyschem* **2010**, *11*, 1871.

(20) El Helou, M.; Medenbach, O.; Witte, G. *Cryst. Growth Des.* **2010**, *10*, 3496.

(21) Menard, E.; Marchenko, A.; Podzorov, V.; Gershenson, M. E.; Fichou, D.; Rogers, J. A. *Adv. Mater.* **2006**, *18*, 1552.

(22) de Boer, R. W. I.; Gershenson, M. E.; Morpurgo, A. F.; Podzorov, V. *Phys. Status Solidi A* **2004**, *201*, 1302.

(23) Yamashita, M. *J. Cryst. Growth* **2008**, *310*, 1739.

(24) Hibino, R.; Nagawa, M.; Hotta, S.; Ichikawa, M.; Koyama, T.; Taniguchi, Y. *Adv. Mater.* **2002**, *14*, 119.

(25) Figi, H.; Jazbinsek, M.; Hunziker, C.; Koechlin, M.; Gunter, P. *Opt. Express* **2008**, *16*, 11310.

(26) Yamao, T.; Miki, T.; Akagami, H.; Nishimoto, Y.; Ota, S.; Hotta, S. *Chem. Mater.* **2007**, *19*, 3748.

(27) Hong, J. P.; Lee, S. *Angew. Chem., Int. Ed.* **2009**, *48*, 3096.

(28) Kloc, C.; Simpkins, P.; Siegrist, T.; Laudise, R. *J. Cryst. Growth* **1997**, *182*, 416.

(29) Laudise, R.; Kloc, C.; Simpkins, P.; Siegrist, T. *J. Cryst. Growth* **1998**, *187*, 449.

(30) Wang, H.; Xie, Z. Q.; Yang, B.; Shen, F. Z.; Li, Y. P.; Ma, Y. G. *Cryst. Eng. Comm.* **2008**, *10*, 1252.

(31) Choubey, A.; Kwon, O. P.; Jazbinsek, M.; Gunter, P. *Cryst. Growth Des.* **2007**, *7*, 402.

(32) Heringdorf, F.; Reuter, M. C.; Tromp, R. M. *Nature* **2001**, *412*, 517.

(33) Davey, R. J.; Allen, K.; Blagden, N.; Cross, W. I.; Lieberman, H. F.; Quayle, M. J.; Righini, S.; Seton, L.; Tiddy, G. J. T. *Cryst. Eng. Comm.* **2002**, 257.

(34) Verlaak, S.; Steudel, S.; Heremans, P.; Janssen, D.; Deleuze, M. S. *Phys. Rev. B* **2003**, *68*.

(35) Zhao, Y. S.; Di, C. A.; Yang, W. S.; Yu, G.; Liu, Y. Q.; Yao, J. N. *Adv. Funct. Mater.* **2006**, *16*, 1985.

(36) Kabe, R.; Nakanotani, H.; Sakanoue, T.; Yahiro, M.; Adachi, C. *Adv. Mater.* **2009**, *21*, 4034.

(37) Nakanotani, H.; Kabe, R.; Yahiro, M.; Takenobu, T.; Iwasa, Y.; Adachi, C. *Appl. Phys. Exp.* **2008**, *1*.

(38) Shimizu, K.; Mori, Y.; Hotta, S. *J. Appl. Phys.* **2006**, 99.

(39) Hibino, R.; Nagawa, M.; Hotta, S.; Ichikawa, M.; Koyama, T.; Taniguchi, Y. *Adv. Mater.* **2002**, *14*, 119.

(40) Ichikawa, M.; Hibino, R.; Inoue, M.; Haritani, T.; Hotta, S.; Koyama, T.; Taniguchi, Y. *Adv. Mater.* **2003**, *15*, 213.

(41) Fujiwara, S.; Bando, K.; Masumoto, Y.; Sasaki, F.; Kobayashi, S.; Haraichi, S.; Hotta, S. *Appl. Phys. Lett.* **2007**, *91*, 021104.

(42) Sasaki, F.; Kobayashi, S.; Haraichi, S.; Fujiwara, S.; Bando, K.; Masumoto, Y.; Hotta, S. *Adv. Mater.* **2007**, *19*, 3653.

(43) Zeng, X. H.; Qiu, Y.; Qiao, J.; Dong, G. F.; Wang, L. D. *Appl. Surf. Sci.* **2007**, *253*, 3581.

(44) Chen, Q. D.; Fang, H. H.; Xu, B.; Yang, J.; Xia, H.; Chen, F. P.; Tian, W. J.; Sun, H. B. *Appl. Phys. Lett.* **2009**, *94*, 201113.

(45) Yanagi, H.; Ohara, T.; Morikawa, T. *Adv. Mater.* **2001**, *13*, 1452.